Proceedings of the ASME 2024 Conference on Smart Materials, Adaptive Structures and Intelligent Systems SMASIS 2024 September 9-11, 2024, Atlanta, GA, USA, USA

SMASIS2024-140453

EXPLORING THE RELATIONSHIP BETWEEN COST FUNCTION OF HYBRID TRAVELING WAVES AND STRUCTURAL REFLECTION COEFFICIENT ADAPTED FROM ACOUSTICS

Samikhshak Gupta[*] **Vijaya V N Sriram Malladi**
VITAL Structures Group,
Department of Mechanical Engineering-Engineering Mechanics
Michigan Technological University
Houghton, Michigan, 49931

ABSTRACT

The Basilar Membrane (BM) is the structural component of the mammalian cochlea that transmits auditory information as traveling structural waves, and inner hair cells transduce acoustic waves into electrical impulses in the inner ear. These waves go up towards the cochlea's apex from its base. The primary structure at the apex of the cochlea that keeps waves from returning to the base is the helicotrema. People can hear continuous sound waves without acoustic reflection or overlap because of this property of the BM. Our research is motivated by this biological phenomenon and aims to comprehend and passively reproduce it in engineering structures. By studying the dynamics of a uniform beam linked to a spring-damper system as a passive absorber, we can use this characteristic of the inner ear to explain some of the observed phenomenological behaviors of the basilar membrane. The spring-damper system's position separates the beam into two dynamic regions: one with standing waves and the other with non-reflecting traveling waves. This study presents the computational realization of traveling waves co-existing with standing waves in the two different zones of the structure. Moreover, this study aims to establish a correlation between two approaches to analyze the characteristics of the wave profiles: (i) the absorption coefficient approach and (ii) the cost function based on the wave envelope. The Basilar Membrane (BM) serves as the crucial structural conduit for transmitting auditory information through traveling structural waves, with inner hair cells in the inner ear transducing these waves into electrical impulses. These waves ascend from the cochlea's base towards its apex, and the helicotrema, positioned at the cochlear apex, plays a pivotal role in preventing wave reflection and overlap, thereby facilitating the perception of continuous sound waves. The intrinsic characteristics of the Basilar Membrane (BM) inspire our research as we seek to comprehend and passively replicate this phenomenon in simplified forms. The investigation involves the exploration of the dynamics exhibited by a uniform beam connected to a spring-damper system acting as a passive absorber. This chosen system allows us to take advantage of the unique property of the inner ear, shedding light on some of the observed phenomenological behaviors of the basilar membrane. The positioning of the spring-damper system engenders two distinct dynamic regions within the beam: one characterized by standing waves and the other by non-reflecting traveling waves. The comprehensive analysis incorporates analytical and computational aspects, providing a holistic understanding of the coexistence of traveling and standing waves within these two dynamic zones.

[*]Address all correspondence to this author.

1 INTRODUCTION

Mechanical waves may be classified according to their capacity to transmit energy as traveling or standing waves. In the case of standing waves, the energy is localized to specific regions, whereas traveling waves can propagate the energy over distances within the medium. Numerous aquatic animals and microbes swim in fluid environments using traveling wave-based locomotion. Researchers have been fascinated by this wave-based locomotion phenomenon for more than five decades. Thus, traveling waves extend across various applications, including the advancement of propulsion mechanisms for robotic locomotion, [1–4], imitation of swimming behaviors [5–7], and the design of biomechanical structures such as the cochlea of the inner ear [8–13], drawing inspiration from microorganisms employing flagella or cilia [14–18], as well as microorganisms such as fish [19–21]. Moreover, traveling waves facilitate the reduction of skin friction drag in aerodynamic structures [22, 23], and enable non-prehensile transportation of macro and micro objects [24–26]. Considering the importance of traveling waves and their many practical uses, researchers have explored ways to create traveling waves in various finite structures. For instance, they have investigated how to generate these waves in strings [27–32], plates [33, 34], rings [35], beams [26, 36–39] and even in circular acoustic conduits with rigid walls [40, 41]. In their examination of mechanical wave characterization and identification, Bucher et al. illustrated that induction of traveling waves within a structure is feasible through a two-point excitation mechanism operating at a mean frequency positioned between two modes, each differing by a 90° phase angle [35]. Malladi and Avirovik et al. employed the previously mentioned two-point excitation approach [26] to generate traveling waves in piezoceramics-augmented 1d beams subjected to a range of boundary conditions [36, 38]. Their research, which included theoretical modeling and experimental validation of traveling wave generation, revealed that each frequency corresponds to a specific phase that contributes to wave formation, thus challenging the notion that this contribution is restricted to the mean frequency and a 90° phase difference. Furthermore, Blanchard et al. explored a novel method for passive motion restriction in fixed strings [30, 31]. Their investigation focused on the dynamics of undamped, uniform, linear strings excited harmonically via an attached spring-dashpot system. Theoretical findings indicate the potential coexistence of stationary and traveling waves due to the complexity of the localized damping-induced mode in the attachment. Accurate estimation of the spring-dashpot system parameters enables passive confinement, facilitating energy transmission to areas with standing waves via traveling waves. Motaharibidgoli et al. [39] devised hybrid waves within an Euler-Bernoulli beam using a single-point excitation technique and integrating a spring damper system. Through this approach, they successfully demonstrated the ability to distinguish between traveling and standing waves while also optimizing wave quality through the utilization of various spring-damper combinations. Furthermore, Xiao et al. [40, 41] used a damped side branch in a circular duct with stiff walls to differentiate between standing and traveling waves. They discovered that the branch efficiently breaks up these waves, transferring or dispersing sound energy without reflecting it to the source. As a result, the technology allows control over energy transmission within the duct by acting as an acoustic confinement mechanism. Denis et al. [42] have demonstrated that traveling waves within a beam can be effectively absorbed by applying a thin layer of damping material to one end of the beam, an effect known as the "Acoustic Black Hole effect." In their study, they investigated the reflection coefficient of the beam under this phenomenon.

Recent studies have highlighted the generation of steady-state traveling waves (SSTW) by adjusting phase differences between several harmonic forces acting on a structure. Although these studies have mostly focused on modal analysis and two-mode excitation to understand the fundamentals of SSTW, one needs to understand further the effect of the spring-dashpot combination in tailoring the two propagating waveforms in a beam. Thus, using finite element (FE) simulations, the main goal of this work is to understand the wave characteristics using the reflection coefficient of SSTW and its relationship to the cost function of hybrid traveling waves produced by a spring damper system attached to a Timoshenko beam.

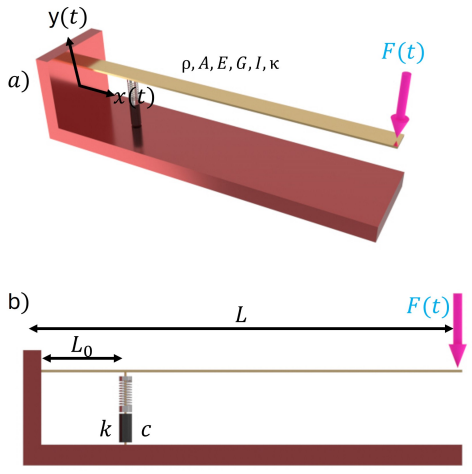

FIGURE 1: Schematic of Cantilever Beam with an attached spring-damper and harmonic force: a) 3D schematic and b) 2D schematic

2 BEAM FORMULATION

A beam of Al 6061-T6 material having a rectangular cross-section of $1.5875 \times 12.7\ mm^2$ and length of $1.5812\ m$ is considered in this study. Using Timoshenko beam formulation, the governing equation of a beam is described as,

$$GA\kappa\left(\frac{\partial\psi(x,t)}{\partial x}-\frac{\partial^2 y(x,t)}{\partial x^2}\right)+\rho A\frac{\partial^2 y(x,t)}{\partial t^2}=q(x,t), \quad (1)$$

$$GA\kappa\left(\frac{\partial y(x,t)}{\partial x}-\psi(x,t)\right)+EI\frac{\partial^2\psi(x,t)}{\partial x^2}=\rho I\frac{\partial^2\psi(x,t)}{\partial t^2}, \quad (2)$$

where G is the shear modulus, A is the area of cross-section, $y(x,t)$ and $\psi(x,t)$ are the transverse displacement and the angle of rotation at location x and time t, q is the load, E is the Young's Modulus, ρ is the density, and I is the moment of inertia. This section provides a concise overview of the modeling approach used to analyze a beam incorporating a spring-damper (SD) system that functions as a passive absorber (PA). The schematic representation of the cantilevered beam, incorporating a discrete spring-damper with stiffness denoted by k [N/m] and damping denoted by c [Ns/m], is shown in Figure 1. The beam is subjected to a harmonic force, $F(t)$, characterized by a driving frequency of ω and an amplitude of F_0, applied at its free end to induce system excitation. Boundary conditions dictate that the displacement $y(x,t)$ and the rotation angle $\psi(x,t)$ are zero at the clamped end of the beam. A MATLAB-based FE model comprising 200 quadratic shape functions has been thoroughly tested and validated in previous research endeavors [43].

$$M\ddot{\mathbf{x}}+C\dot{\mathbf{x}}+K\mathbf{x}=B_f f(t) \quad (3)$$

where the mass, stiffness, and damping matrices are given by $M,K,C\in\mathbb{R}^{800\times800}$. Also, C can be written in terms of $M\&K$ as shown below Equation (4).

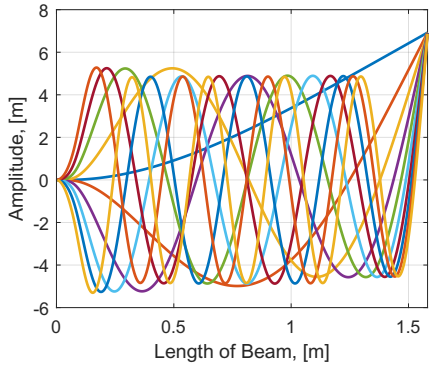

FIGURE 2: Modified Modeshapes of the Beam after adding Spring-Damper

$$C=\alpha M+\beta K \quad (4)$$

here, $\alpha=1e^{-3}$ and $\beta=1e^{-6}$ are FE constants used from the FE model from previous research [43]. In particular, a thorough analysis verified that natural frequencies converged within the applicable frequency range. The spring-damper assembly is attached at position $L_0=0.05L$, and the resulting modified modeshapes are illustrated in Figure 2.

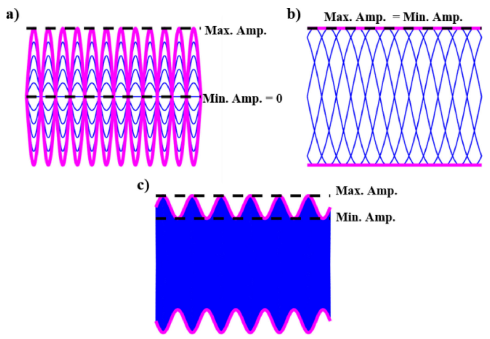

FIGURE 3: Illustration of wave types by (CF): (a) Pure Standing wave (CF=1), (b) Pure Traveling wave (CF=0), and (c) Hybrid wave (0<CF<1)

3 WAVE CATEGORIZATION

To assess the quality of a wave generated within a structural context and to delineate its waveform characteristics, a cost function (CF) is used, based on the wave envelope [37].

$$CF=\frac{MaxAmp-MinAmp}{MaxAmp+MinAmp} \quad (5)$$

Within this framework, the parameters $MaxAmp$ and $MinAmp$ denote the maximal and minimal amplitudes of the wave envelope within a predetermined time interval, as shown in Figure 3. The CF, as illustrated in Figure 3and formulated by Equation (5), assumes values ranging between zero and one, where a CF of zero signifies a purely propagating wave, while a CF of one indicates a purely standing wave. A wave exhibiting a CF within the interval (0, 1) denotes a composite of propagating and standing wave components. It is pertinent to acknowledge that attaining a CF value of precisely zero within mechanical media, as examined herein, may not be feasible. A hypothetical situation, which serves as an example but is not realistically achievable, involves envisioning a scenario where a string with no constraints experiences forces acting on both ends. Consequently, as the CF approaches zero, a hybrid wave progressively resembles a propagating rather than a standing wave.

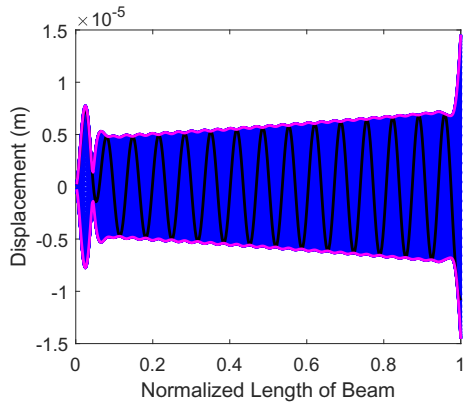

(a) Hybrid Wave generated in the system for ω = 1700 Hz, L_0 = 0.05L

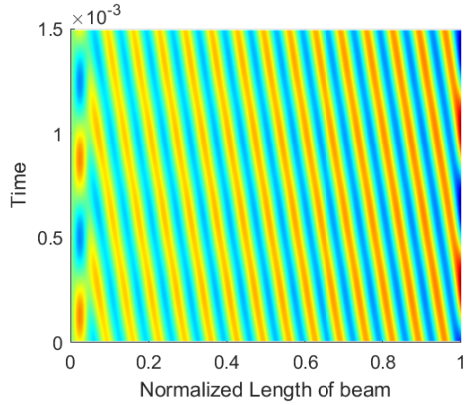

(b) Surface Plot for the above traveling wave

4 NUMERICAL SIMULATIONS AND OPTIMIZATION

MATLAB software is utilized to solve the equation of motion Equation (6) employing the inverse matrix technique.

$$M\ddot{\mathbf{x}} + (C + cB_{sd})\dot{\mathbf{x}} + (K + kB_{sd})\mathbf{x} = B_f f(t) \tag{6}$$

where, $\mathbf{x}$ is the displacement vector of the beam, M, C and K are global mass, damping and stiffness matrices, c and k are the damping and stiffness coefficient of the SD, respectively, $f(t)$ is the input force applied to the free end of the beam, B_f is the force influence matrix and B_{sd} is the spring-damper influence matrix. Once the displacement has been computed, Equation (5) is applied to obtain the Cost Function for the traveling wave. Figure 4a depicts a hybrid wave applied to the clamped-free beam at an excitation frequency 1300 Hz while Figure 4b illustrates a contour plot showcasing the presence of both standing wave and traveling wave across the length of the beam.

Additionally, the parameters k and c are optimized so that the cost function corresponding to a specific excitation frequency is minimized. As illustrated in Figure 5, a contour plot elucidates the correlation between the cost function and the span of c and k.

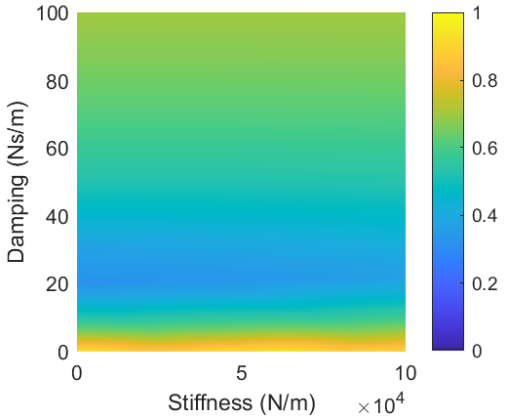

FIGURE 5: Cost Function contour for the system excited at ω = 1300 Hz for a range of k and c

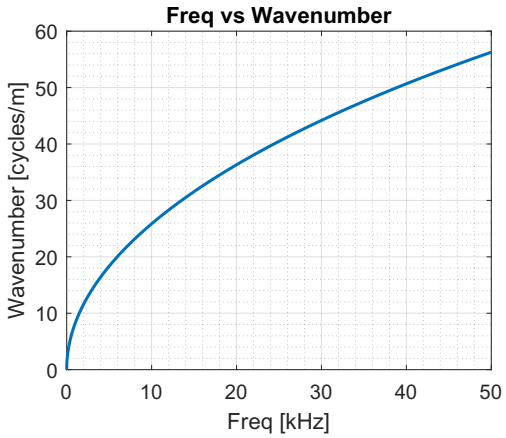

FIGURE 6: Wave Number v/s Frequency

5 WAVE FIELD SOLUTION AND ESTIMATION OF REFLECTION COEFFICIENT FOR BEAM

Given the identical beam model incorporating a spring-damper system that resembles an acoustic black hole affixed to the extremity, located at $x = 0.05L$, where L represents the beam length. Under the Timoshenko beam assumptions the equation of the flexural motion Equation (7), $\mathbf{W}(x,\omega)$ of such a beam in the absence of excitation and harmonic motion with time dependency $e^{-j\omega t}$, is

$$\frac{EI}{\rho A}{k_f}^4 - \frac{I}{A}\left(1 + \frac{E}{G\kappa}\right){k_f}^2\omega^2 - \omega^2 + \frac{\rho I}{GA\kappa}\omega^4 = 0 \tag{7}$$

where κ is the Timoshenko Coefficient, ω is the angular frequency, ρ is the density, E is the Young's Modulus, G is the shear modulus, A is the area of cross-section, I is the Moment of

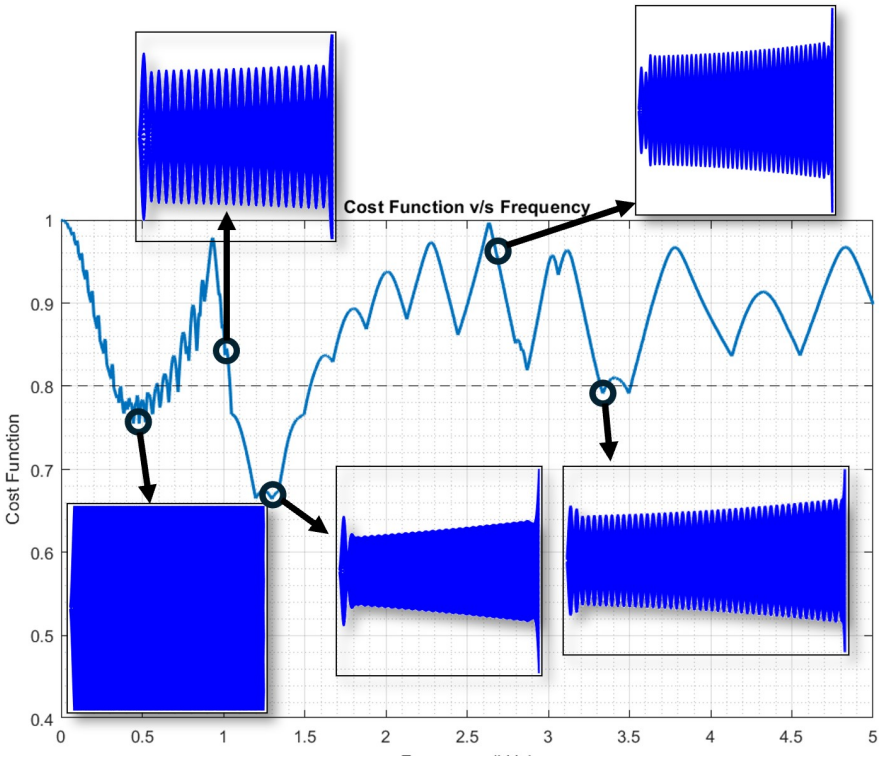

FIGURE 7: Cost Function v/s Frequency for L_0 = 0.05L

Inertia for the beam respectively.

The overall solution for the displacement can be expressed as the summation of four distinct waves [44]:

$$\mathbf{W}(x) = Ae^{-jk_f x} + Be^{+jk_f x} + Ce^{-k_f x} + D(\omega)e^{+k_f x} \tag{8}$$

where k_f is the spatial frequency, i.e., wave number. The roots of the wave number vary with the angular frequency as shown in Figure 6. The wave number for a particular frequency is determined by solving the dispersion relationship shown in Equation (7).

This is subsequently employed in the determination of scalar coefficients. A, B, C, and D signify the complex amplitudes of backward and forward propagating waves, respectively. At the extremities, the boundary conditions associated with the equation of motion Equation (7) can be formulated in the form of a reflection matrix denoted as $\mathbf{R}$, [42] such that

$$\begin{bmatrix} A \\ C \end{bmatrix} = \mathbf{R} \begin{bmatrix} B \\ D \end{bmatrix} \tag{9}$$

where

$$\mathbf{R} = \begin{bmatrix} R_{pp} & R_{ap} \\ R_{pa} & R_{aa} \end{bmatrix} \tag{10}$$

with R_{ij} being the reflection coefficient between incident wave i and reflected wave j; i and j symbolize p and a standing for propagating and attenuating, respectively. Considering 25 points along the beam, the displacement measured for all $x_i (i \in [0, N])$ can be related to the coefficients A, B, C, D through the matrix equation

$$\begin{bmatrix} W(x_0,\omega) \\ W(x_1,\omega) \\ W(x_2,\omega) \\ \vdots \\ W(x_{25},\omega) \end{bmatrix} = \begin{bmatrix} e^{-jk_f x_0} & e^{+jk_f x_0} & e^{-k_f x_0} & e^{+k_f x_0} \\ e^{-jk_f x_1} & e^{+jk_f x_1} & e^{-k_f x_1} & e^{+k_f x_1} \\ e^{-jk_f x_2} & e^{+jk_f x_2} & e^{-k_f x_2} & e^{+k_f x_2} \\ \vdots & \vdots & \vdots & \vdots \\ e^{-jk_f x_{25}} & e^{+jk_f x_{25}} & e^{-k_f x_{25}} & e^{+k_f x_{25}} \end{bmatrix} \begin{bmatrix} A(\omega) \\ B(\omega) \\ C(\omega) \\ D(\omega) \end{bmatrix} \tag{11}$$

$$\begin{bmatrix} A(\omega) \\ B(\omega) \\ C(\omega) \\ D(\omega) \end{bmatrix} = M^{\dagger} \begin{bmatrix} W(x_0,\omega) \\ W(x_1,\omega) \\ W(x_2,\omega) \\ \vdots \\ W(x_{25},\omega) \end{bmatrix} \tag{12}$$

where,

$$M^{\dagger} = (M^{*}M)^{-1}M^{*} \tag{13}$$

$M^{\dagger}$ is the Moore-Penrose generalized inverse [42] of M and M^{*} is the conjugate transpose of M

Then, the Reflection coefficient

$$R(\omega) = \frac{A(\omega)}{B(\omega)} \tag{14}$$

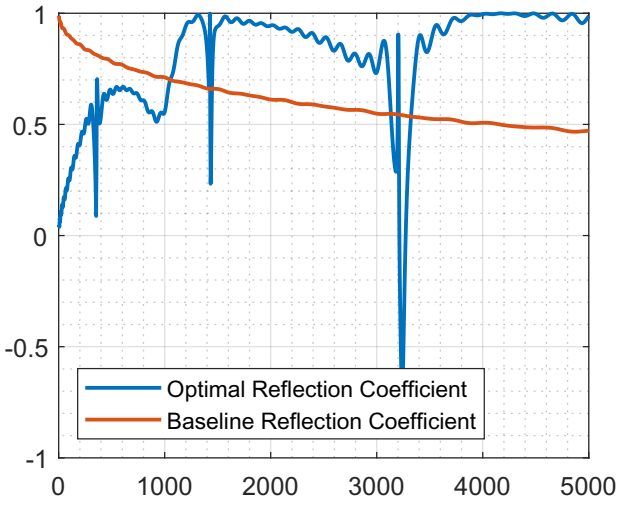

FIGURE 8: Reflection Coefficient when SD is at $L_0 = 0.05$L

6 DISCUSSION & CONCLUSION

Our research has yielded a significant discovery: Depicted in Figure 7, our analysis reveals distinct troughs in the cost function spanning a wide frequency spectrum. Specifically, we examine a spring-damper system situated at $L_0 = 0.05^{*}L$, with L denoting the normalized length, and tailor it for a frequency of 1340 Hz in Figure 7. This optimization underscores the pronounced dips in the cost function. This revelation hints at an extraordinary prospect: a singular system might concurrently sustain traveling waves across multiple frequencies, which is a novel observation and not previously documented. In particular, in Figure 7, we set a threshold for the cost function at 0.8, revealing several peaks below this criterion. Intriguingly, these troughs manifest between two natural frequencies, challenging conventional assumptions and beckoning a deeper examination of the mechanisms governing wave propagation dynamics.

Expanding on this revelation, our investigation uncovers a compelling correlation between dips in the cost function and corresponding decreases in the reflection coefficient across diverse frequency bands (Figure 8). We discern that both metrics exhibit a dip at the same natural frequency optimized for the spring-damper system. This intriguing correlation underscores an inherent link between the system's wave propagation characteristics and dynamic behavior. Beyond enriching our understanding of wave phenomena, this insight holds significant implications for engineering disciplines, offering new avenues for system design and optimization.

7 FUTURE SCOPE

In future studies, there exists a promising avenue for actively manipulating these observed dips to enhance system efficiency. Rather than merely accommodating dips, the aim would be to minimize the cost function to a singular minimum across a wide frequency spectrum. Exploring this prospect could yield valuable insights into optimizing system performance. Moreover, delving into potential applications within cutting-edge wave-based technologies and materials design holds substantial promise.

Furthermore, it is imperative to delve deeper into the underlying mechanisms driving the correlation between system dynamics and wave propagation characteristics. Clarifying these intricacies would not only enrich our fundamental understanding but also lay the groundwork for future innovation and advancement in the field. By embarking on these paths of inquiry, we can unlock novel opportunities for pushing the boundaries of scientific exploration and practical application.

8 ACKNOWLEDGEMENT

The authors (VVNSM and SG) would like to thank the support of the National Science Foundation through the grant CMMI-2301776 for sponsoring the research presented in this paper.

REFERENCES

[1] Kalani, H., Akbarzadeh, A., and Safehian, J., 2010. "Traveling wave locomotion of snake robot along symmetrical and unsymmetrical body shapes". In ISR 2010 (41st International Symposium on Robotics) and ROBOTIK 2010 (6th German Conference on Robotics), VDE, pp. 1–7.

[2] Chen, L., Ma, S., Wang, Y., Li, B., and Duan, D., 2007. "Design and modelling of a snake robot in traveling wave locomotion". *Mechanism and Machine Theory,* ***42***(12), pp. 1632–1642.

[3] Haomachai, W., Dai, Z., and Manoonpong, P., 2024. "Transition gradient from standing to traveling waves for energy-

efficient slope climbing of a gecko-inspired robot". *IEEE Robotics and Automation Letters*.

[4] Salem, L., Gat, A. D., and Or, Y., 2022. "Fluid-driven traveling waves in soft robots". *Soft Robotics,* ***9***(6), pp. 1134–1143.

[5] Du, R., Li, Z., Youcef-Toumi, K., and y Alvarado, P. V., 2015. *Robot fish: Bio-inspired fishlike underwater robots*. Springer.

[6] Erturk, A., and Delporte, G., 2011. "Underwater thrust and power generation using flexible piezoelectric composites: an experimental investigation toward self-powered swimmer-sensor platforms". *Smart materials and Structures,* ***20***(12), p. 125013.

[7] Syuhri, S. N., Pickles, D., Zare-Behtash, H., and Cammarano, A., 2023. "Influence of travelling waves on the fluid dynamics of a beam submerged in water". *Journal of Fluids and Structures,* ***121***, p. 103947.

[8] Davaria, S., and Tarazaga, P. A., 2017. "Mems scale artificial hair cell sensors inspired by the cochlear amplifier effect". In Bioinspiration, Biomimetics, and Bioreplication 2017, Vol. 10162, SPIE, pp. 82–91.

[9] Davaria, S., Malladi, V. V. S., Motaharibidgoli, S., and Tarazaga, P. A., 2019. "Cochlear amplifier inspired two-channel active artificial hair cells". *Mechanical Systems and Signal Processing,* ***129***, pp. 568–589.

[10] Hubbard, A., 1993. "A traveling-wave amplifier model of the cochlea". *Science,* ***259***(5091), pp. 68–71.

[11] Davaria, S., Sriram Malladi, V., and Tarazaga, P. A., 2019. "Bio-inspired nonlinear control of artificial hair cells". In Structural Health Monitoring, Photogrammetry & DIC, Volume 6: Proceedings of the 36th IMAC, A Conference and Exposition on Structural Dynamics 2018, Springer, pp. 179–184.

[12] Davaria, S., and Tarazaga, P. A., 2022. "Toward developing arrays of active artificial hair cells". In Special Topics in Structural Dynamics & Experimental Techniques, Volume 5: Proceedings of the 39th IMAC, A Conference and Exposition on Structural Dynamics 2021, Springer, pp. 75–80.

[13] Johnstone, B., Patuzzi, R., and Yates, G., 1986. "Basilar membrane measurements and the travelling wave". *Hearing research,* ***22***(1-3), pp. 147–153.

[14] Machin, K., 1958. "Wave propagation along flagella". *Journal of Experimental Biology,* ***35***(4), pp. 796–806.

[15] Brokaw, C., 1965. "Non-sinusoidal bending waves of sperm flagella". *Journal of Experimental Biology,* ***43***(1), pp. 155–169.

[16] Brokaw, C. J., 1972. "Flagellar movement: a sliding filament model: an explanation is suggested for the spontaneous propagation of bending waves by flagella.". *Science,* ***178***(4060), pp. 455–462.

[17] Rikmenspoel, R., 1965. "The tail movement of bull spermatozoa: observations and model calculations". *Biophysical journal,* ***5***(4), pp. 365–392.

[18] Taylor, G. I., 1952. "The action of waving cylindrical tails in propelling microscopic organisms". *Proceedings of the Royal Society of London. Series A. Mathematical and Physical Sciences,* ***211***(1105), pp. 225–239.

[19] Sfakiotakis, M., Lane, D. M., and Davies, J. B. C., 1999. "Review of fish swimming modes for aquatic locomotion". *IEEE Journal of oceanic engineering,* ***24***(2), pp. 237–252.

[20] Liu, F., Lee, K.-M., and Yang, C.-J., 2011. "Hydrodynamics of an undulating fin for a wave-like locomotion system design". *IEEE/ASME Transactions on Mechatronics,* ***17***(3), pp. 554–562.

[21] Kancharala, A., and Philen, M., 2014. "Enhanced hydrodynamic performance of flexible fins using macro fiber composite actuators". *Smart materials and structures,* ***23***(11), p. 115012.

[22] Musgrave, P. F., Sriram Malladi, V., and Tarazaga, P. A., 2016. "Generation of traveling waves in a 2d plate for future drag reduction manipulation". In Special Topics in Structural Dynamics, Volume 6: Proceedings of the 34th IMAC, A Conference and Exposition on Structural Dynamics 2016, Springer, pp. 129–138.

[23] Musgrave, P. F., and Tarazaga, P. A., 2017. "Skin friction drag reduction in turbulent flow using spanwise traveling surface waves". Vol. 10164. Cited by: 4.

[24] Loh, B.-G., and Ro, P., 2000. "An object transport system using flexural ultrasonic progressive waves generated by two-mode excitation". *IEEE Transactions on Ultrasonics, Ferroelectrics, and Frequency Control,* ***47***(4), pp. 994–999.

[25] Fu, L.-M., Lee, G.-B., Lin, Y.-H., and Yang, R.-J., 2004. "Manipulation of microparticles using new modes of traveling-wave-dielectrophoretic forces: numerical simulation and experiments". *IEEE/ASME Transactions on Mechatronics,* ***9***(2), pp. 377–383.

[26] Loh, B.-G., and Ro, P. I., 2000. "An object transport system using flexural ultrasonic progressive waves generated by two-mode excitation". *IEEE transactions on ultrasonics, ferroelectrics, and frequency control,* ***47***(4), pp. 994–999.

[27] Anakok, I., 2018. "A study on steady state traveling waves in strings and rods". PhD thesis, Virginia Tech.

[28] Anakok, I., Malladi, V. S., and Tarazaga, P. A., 2019. "A study on the generation and propagation of traveling waves in strings". In Topics in Modal Analysis & Testing, Volume 9: Proceedings of the 36th IMAC, A Conference and Exposition on Structural Dynamics 2018, Springer, pp. 257–261.

[29] Anakok, I., Malladi, V. S., and Tarazaga, P. A., 2020. "A theoretical study on the generation and propagation of traveling waves in strings". In Topics in Modal Analysis & Testing, Volume 8: Proceedings of the 37th IMAC, A Conference and Exposition on Structural Dynamics 2019,

Springer, pp. 311–316.

[30] Blanchard, A., Gendelman, O. V., McFarland, D. M., Bergman, L. A., and Vakakis, A. F., 2015. "Mode complexity in a harmonically forced string with a local spring–damper and transitions from vibrations to waves". *Journal of Sound and Vibration,* ***334***, pp. 282–295.

[31] Blanchard, A., McFarland, D., Bergman, L., and Vakakis, A., 2015. "Damping-induced interplay between vibrations and waves in a forced non-dispersive elastic continuum with asymmetrically placed local attachments". *Proceedings of the Royal Society A: Mathematical, Physical and Engineering Sciences,* ***471***(2176), p. 20140402.

[32] Anakok, I., Davaria, S., Tarazaga, P. A., and Malladi, V. V. S., 2022. "A study on steady-state traveling waves in one-dimensional non-dispersive finite media". *Journal of Sound and Vibration,* ***528***, p. 116907.

[33] Malladi, V. V. S., Albakri, M., and Tarazaga, P. A., 2017. "An experimental and theoretical study of two-dimensional traveling waves in plates". *Journal of Intelligent Material Systems and Structures,* ***28***(13), pp. 1803–1815.

[34] Musgrave, P. F., Albakri, M. I., Tenney, C., and Tarazaga, P. A., 2020. "Generating and tailoring structure-borne traveling waves on two-dimensional surfaces". *Journal of Sound and Vibration,* ***480***, p. 115417.

[35] Bucher, I., 2004. "Estimating the ratio between travelling and standing vibration waves under non-stationary conditions". *Journal of sound and vibration,* ***270***(1-2), pp. 341–359.

[36] Avirovik, D., Malladi, V. S., Priya, S., and Tarazaga, P. A., 2016. "Theoretical and experimental correlation of mechanical wave formation on beams". *Journal of Intelligent Material Systems and Structures,* ***27***(14), pp. 1939–1948.

[37] Cheng, X., Bergman, L. A., McFarland, D. M., Tan, C. A., Vakakis, A. F., and Lu, H., 2019. "Co-existing complexity-induced traveling wave transmission and vibration localization in euler-bernoulli beams". *Journal of Sound and Vibration,* ***458***, pp. 22–43.

[38] Malladi, V., Avirovik, D., Priya, S., and Tarazaga, P., 2015. "Characterization and representation of mechanical waves generated in piezo-electric augmented beams". *Smart Materials and Structures,* ***24***(10), p. 105026.

[39] Motaharibidgoli, S., Davaria, S., Sriram Malladi, V. V., and Tarazaga, P. A., 2023. "Developing coexisting traveling and standing waves in euler-bernoulli beams using a single-point excitation and a spring-damper system". *Journal of Sound and Vibration,* ***556***, p. 117728.

[40] Xiao, Y., Blanchard, A., Zhang, Y., Lu, H., Michael McFarland, D., Vakakis, A. F., and Bergman, L. A., 2017. "Separation of traveling and standing waves in a rigid-walled circular duct containing an intermediate impedance discontinuity". *Journal of Vibration and Acoustics,* ***139***(6), p. 061001.

[41] Xiao, Y., Lu, H., McFarland, D. M., Vakakis, A. F., and Bergman, L. A., 2018. "Inducing a nonreflective airborne discontinuity in a circular duct by using a nonresonant side branch to create mode complexity". *The Journal of the Acoustical Society of America,* ***143***(2), pp. 746–755.

[42] Denis, V., Gautier, F., Pelat, A., and Poittevin, J., 2015. "Measurement and modelling of the reflection coefficient of an acoustic black hole termination". *Journal of Sound and Vibration,* ***349***, pp. 67–79.

[43] Malladi, V. V. S., Albakri, M. I., Krishnan, M., Gugercin, S., and Tarazaga, P. A., 2022. "Estimating experimental dispersion curves from steady-state frequency response measurements". *Mechanical Systems and Signal Processing,* ***164***, p. 108218.

[44] Mace, B., 1984. "Wave reflection and transmission in beams". *Journal of sound and vibration,* ***97***(2), pp. 237–246.